Effects of reducing agents on the degradation of 2,4,6-tribromophenol in a heterogeneous Fenton-like system with an iron-loaded natural zeolite

Shigeki Fukuchi, Ryo Nishimoto, Masami Fukushima* and Qianqian Zhu

Laboratory of Chemical Resources, Division of Sustainable Resources Engineering, Graduate School of Engineering, Hokkaido University, Sapporo 060-6828, Japan

*Corresponding author. Tel./fax: +81-11-706-6304. E-mail address: m-fukush@eng.hokudai.ac.jp (M. Fukushima)

Abstract

The effects of reducing agents on the degradation of 2,4,6-tribromophennol (TrBP) were investigated in a heterogeneous Fenton-like system using an iron-loaded natural zeolite (Fe-Z). The catalytic activity for TrBP oxidation in the presence of the Fe-Z and H_2O_2 was not appreciable. The addition of a reducing agent, such as ascorbic acid (ASC) or hydroxylamine (NH_2OH), resulted in an enhancement in the degradation and debromination of TrBP. TrBP was completely degraded and debrominated at pH 3 and 5 in the presence of NH_2OH, while the degradation was significantly suppressed at pH 7 and 9. Although the rates of TrBP degradation were relatively constant at pH 3, 5, 7 and 9 in the presence of ASC, the percent degradation reached a plateau at 70%. These results show that ASC functions as a strong $HO^{\bullet}$ scavenger, as opposed to NH_2OH, at pH 3 and 5. Thus, adding NH_2OH is preferable for the degradation of TrBP via a Fenton-like system using Fe-Z as the catalyst. It is noteworthy that the complete mineralization of TrBP was achieved at pH 5, when NH_2OH and H_2O_2 were sequentially added to the reaction mixture. Analysis of the surface of Fe-Z by X-ray

photoelectron spectrometry indicated that the Fe(III) on the surface of the catalyst was reduced to Fe(II) after treatment with ASC. Thus, the role of RAs can be of assistance in Fe(III)/Fe(II) redox cycles on the Fe-Z surface and enhance the generation of $HO^{\bullet}$ via the decomposition of H_2O_2.

Keywords: Fe-loading; Natural zeolite; 2,4,6-Tribromophenol; Heterogeneous Fenton system; Reducing agents

1. Introduction

2,4,6-Tribromophenol (TrBP) is used in the manufacturing of TVs, computers and other household electric appliances as a flame retardant intermediate. As a result of extensive use, TrBP can be found in soils, landfill leachates and sewage sludge [1]. TrBP could have an endocrine disrupting activity *in vivo*, because it has been shown to interfere with the thyroid hormone system by competitive binding to transport proteins [2]. In terms of reducing the potential for pollution and related health issues, it is important to develop the techniques for the oxidative degradation of TrBP in contaminated environments. However, bromophenols are more difficult to oxidize than other halogenated phenols, such as fluorophenols and chlorophenols [3].

Fenton and Fenton-like processes have been the focus of studies dealing with the oxidative degradation of organic pollutants. In such systems, H_2O_2 is catalytically decomposed by Fe(II) to generate a powerful oxidant, the hydroxyl radical ($HO^{\bullet}$). The overall process is referred to the Haber-Weiss reaction as below [4]:

$$Fe(II) + H_2O_2 \rightarrow Fe(III) + HO^{\bullet} + OH^{-} \quad (k = 63\ M^{-1}\ s^{-1}\ [5]) \qquad (1)$$

Numerous studies related to the degradation of chlorophenols by homogeneous Fenton

and Fenton-like systems have appeared [6-8], but much less information is available concerning the degradation of bromophenols. The homogeneous Fenton processes is limited to the pH range from 2.5 to 3.5, because Fe(III)-hydroxides are converted into sludge, leading to the deactivation of catalytic activity for oxidation [9]. To overcome such problems, heterogeneous Fenton-like systems in which Fe(II) or Fe(III) are supported to a solid support have been examined: *e.g.*, minerals [10-13] and cation exchange resins [14, 15].

In particular, Fe-loaded zeolites have been demonstrated to function as active catalysts in the degradation of organic pollutants in the presence of H_2O_2 [16-21]. In these studies, synthesized zeolites such as Y-, ZSM-5 and Beta zeolites were mainly employed and Fe^{2+} or Fe^{3+} were loaded via cation-exchange reactions. Although natural zeolites are cheap and widely distributed, they have not been used extensively as catalysts, but are mainly utilized as adsorbents [22] and soil amendments [23-25]. The surface areas of natural zeolites (16 – 38 m^2 g^{-1}) [22-25] are much smaller than those the synthesized materials (300 – 800 m^2 g^{-1}) [17-21], because of the presence of impurities such as quartz and feldspar. Such smaller surface areas of natural zeolites may be a disadvantage in terms of achieving a higher catalytic activity.

In homogeneous system, Fenton and Fenton-like systems combined with light irradiation [7, 8, 26] and electrochemical processes [27] have been examined to accelerate the redox cycle of Fe(III)/Fe(II) and the generated $HO^{\bullet}$. Although the addition of reducing agents (RAs) seems to be simple and effective in accelerating the reduction of Fe(III) to Fe(II), they may also serve as inhibitors of oxidative Fenton processes because of their oxidation by $HO^{\bullet}$. It has, however, been reported that the addition of RAs, such as ascorbic acid (ASC) and hydroxylamine (NH_2OH), to

73 homogeneous Fenton-like systems can be effective in enhancing the generation of $HO^{\bullet}$,
74 ultimately leading to the degradation of organic substrates [28-30]. In the present study,
75 the addition of RAs, such as ASC, NH_2OH, *p*-hydroquinone, oxalic, gallic and humic
76 acids, to a heterogeneous Fenton-like system with an iron-loaded natural zeolite (Fe-Z)
77 was examined. The reactivity of the heterogeneous Fenton-like system was evaluated
78 using the oxidative degradation of TrBP as a model system.
79
80 **2. Materials and Methods**
81 *2.1. Materials*
82 ASC, NH_2OH, *p*-hydroquinone, oxalic and gallic acids, employed as RAs, were
83 purchased from Nacalai Tesque (Kyoto, Japan). The humic acid, a natural RA, was
84 extracted from a Shinshinotsu peat soil sample (Hokkaido, Japan), as described in a
85 previous report [31]. TrBP (98 % purity) was purchased from Tokyo Chemical Industry
86 (Tokyo, Japan), and a stock solution (0.01 M) was prepared by dissolving it in 0.02 M
87 NaOH. The standard sample of 2,6-dibromo-*p*-benzoquinone (2,6DBQ) was
88 synthesized according to a previous report [32]. A natural zeolite sample was obtained
89 from the town of Niki (Hokkaido, Japan). All other reagents were purchased from Wako
90 Pure Chemicals (Osaka, Japan) and were used without further purification. The
91 ultra-pure water, prepared by a Millipore ultra-pure system from distilled water, was
92 used in all experiments.
93
94 *2.2. Synthesis of Fe-Z*
95 The cation-exchange capacities (CECs) for each sample were determined, as
96 described in a previous report [23], and the CEC of the natural zeolite was determined

97 to be 170 ± 7 (cmol kg^{-1}), as shown in Table 1. The zeolite powder was stirred in
98 aqueous $FeSO_4$ $(NH_4)_2SO_4 \cdot 6H_2O$ under a N_2 atmosphere at room temperature for 72
99 hours, in which the amount of iron was adjusted to the equivalent mole of CEC for the
100 zeolite. After filtration of the slurry, the resulting solid was washed with distilled water
101 and then freeze-dried. The powder was calcined at 500 ºC for 8 h to obtain the
102 Fe-loaded catalyst (Fe-Z). The inorganic element compositions (Al, Si, Ca and Fe) and
103 specific surface areas (SSAs) for the original zeolite and Fe-Z were determined, as
104 described in a previous report [24]. As shown in Table 1, the iron content (wt %) in the
105 Fe-Z was 1.54±0.06%, corresponding to be 276±11 μmol-Fe g^{-1}. In the present study,
106 this was considered to be moles of catalytic sites in the Fe-Z. The specific surface areas
107 (SSAs), total pore volume and pore size were determined by a N_2-BET method using a
108 BECKMAN COULTER SA3100-type instrument.
109
110 *2.3. Assay for the reaction mixture*
111 Test solutions, which contained TrBP (100 μM) and the RAs (0.25 – 10 mM) at pH 3,
112 5, 7 or 9, were prepared, and 30 mL aliquots of these solutions were then placed in a
113 100-mL Erlenmeyer flask that contained powdered Fe-Z (2.7 – 54.2 mg). After adding
114 an aqueous solution of H_2O_2 (0.25 – 100 mM), the reaction mixture was subjected to
115 shaking at 25ºC. During the reaction period, an 800 μL aliquot of the test solution was
116 withdrawn and then mixed with a 400 μL of 2-propanol, followed by vigorous mixing.
117 After centrifugation, a 20 μL aliquot of the supernatant was injected into a PU-980 type
118 HPLC system (Japan Spectroscopic Co., Ltd.) to determine the concentration of the
119 residual TrBP in the reaction mixture. The detailed conditions for the HPLC analysis are
120 described in Supplementary data (Text S1). When 2-propanol was added to a mixture of

TrBP and Fe-Z without H_2O_2, nearly 100% of the TrBP was recovered. However, in the absence of 2-propanol, only 2 – 3% of the TrBP was adsorbed to Fe-Z. Thus, the adsorption of TrBP to the Fe-Z is negligible. The concentration of Br^- in the reaction mixture was analyzed by a DX-120 type ion chromatography (Dionex).

The oxidation products, such as 2,6DBQ, that were produced in the reaction were acetylated, and these resulting acetyl derivatives were analyzed using a GC/MS system after extraction with *n*-hexane. The detailed procedures are described in Supplementary data (Text S2). The mass spectra of the detected peaks were assigned based on peaks for fragmentation ions.

In the test for TrBP mineralization, aqueous mixtures containing 5 mM NH_2OH and 100 μM TrBP at pH 3, 5, 7 or 9 were prepared, and 30 mL aliquots of these solutions were placed to the 100-mL Erlenmeyer flask that contained 13.1 mg of Fe-Z. After adding a 150 μL aliquot of 1 M aqueous H_2O_2, the flask was allowed to shake for 180 min. After the reaction, a 20 mL aliquot of the reaction mixture was mixed with 1 M aqueous Na_2SO_3 (1 mL), and the TOC of the solution was analyzed using a TOC-V CSH-type analyzer (Shimadzu).

The consumption of H_2O_2 during the reaction was monitored using a 30-mL aliquot of the reaction mixture, which contained H_2O_2 (5 mM) and Fe-Z (436 mg L^{-1} for NH_2OH and 216 mg L^{-1} for ASC) in the absence and presence of RAs (5 mM for NH_2OH and 7 mM for ASC) at pH 3 and 9. A 200-μL aliquot of the reaction mixture was withdrawn and transferred to a 1.5-mL centrifuge tube. After centrifugation, a 10 μL aliquot of the supernatant was diluted to 5 mL with pure water. The H_2O_2 in this solution was quantitatively determined by an *N*,*N*,-diethyl-*p*-phenylenediamine colorimetry [33].

145 The iron in the reaction mixture, eluted from the Fe-Z after a 180 min period, was
146 analyzed by ICP-AES after filtering the reaction mixture through a membrane filter
147 (0.45 μm).
148
149 *2.4. X-ray photoelectron spectrometry*
150 XPS spectra were recorded using a JEOL JPC-9500F-type XPS spectrometer with
151 Mg Kα radiation. The dried powdered sample was placed on a carbon tape attached to
152 an aluminum sample holder. Before recording the XPS, the catalysts were evacuated in
153 the XPS analyzer chamber. The pressure in the analysis chamber was maintained at less
154 than 3.00×10^{-6} Pa. The analyzer was operated at a pass energy of 10 eV. The biding
155 energy (BE) for Fe was referenced to the Si(2p) peak at 102.8 eV as an internal
156 standard.
157
158 **3. Results and Discussion**
159 *3.1. Characterization of the original zeolite sample and Fe-Z*
160 The Elemental composition, pore volume, particle size distribution, CEC and specific
161 surface areas (SSAs), total pore volume and average pore diameter for the original
162 zeolite and Fe-Z are summarized in Table 1. The Si/Al molar ratio of the original zeolite
163 (15.6) remained constant compared to that for the Fe-Z (15.6). The CEC value for the
164 Fe-Z was significantly smaller than that for the original zeolite, indicating that Fe binds
165 tightly to the cation-exchange sites on the surface of the zeolite. The XRD patterns,
166 shown in the Supplementary data section (Fig. S1), indicated that the minerals for the
167 original zeolite and Fe-Z samples were clinoptilolite [$(Na,K,Ca)_4(Si_{30}Al_6)O_{72}\bullet24H_2O$]
168 and mordenite [$(Na,K,Ca)(Si_{10}Al_2)O_{24}\bullet7H_2O$], and the structural type was consistent

169 with the typical natural zeolite heulandite (HEU) [34]. The SSAs for the original zeolite
170 (24.7 m^2 g^{-1}) and Fe-Z (29.2 m^2 g^{-1}) were much smaller than those for the pure zeolites
171 (300 – 800 m^2 g^{-1}) [17-21], indicating that the original zeolite and Fe-Z samples
172 contained impurities. The content of zeolite in the original zeolite and Fe-Z was
173 estimated to be 4 – 10% by comparison with the reported SSAs for pure zeolites.
174
175 *3.2. Influence of RAs on the kinetics of TrBP degradation*
176 The majority of RAs can serve as $HO^{\bullet}$ scavengers, leading to the inhibition of
177 substrate oxidation via Fenton processes [35]. However, quinones have been reported to
178 serve as electron shuttles for assisting Fe(III)/Fe(II) redox cycles in homogeneous
179 Fenton-like processes [36], and humic acids, naturally occurring polyphenols, are also
180 able to reduce Fe(III) [37]. In addition, oxalic acid, ASC and NH_2OH are known as
181 strong RAs that are used for the reduction of Fe(III) [39, 39]. Thus, the addition of these
182 RAs was first examined for the degradation of TrBP via the heterogeneous Fenton-like
183 system with the Fe-Z catalyst at pH 3.
184 Figure 1 shows the degradation kinetics of TrBP in the presence and absence of RAs.
185 In the presence of Fe-Z alone without RAs (g in Fig. 1), only 5% of the TrBP was
186 degraded during a 180 min period, even in the presence of H_2O_2 (20 mM). For the
187 controls without H_2O_2 and in the presence of H_2O_2 without the Fe-Z catalyst, no TrBP
188 disappearance was observed. In Haber-Weiss processes leading to the generation of
189 $HO^{\bullet}$ by the catalytic decomposition of H_2O_2 (eq 1), the Fe(III) species can be reduced
190 to Fe(II) by H_2O_2 and $HO_2^{\bullet}$, as shown below [36]:

191 $$Fe(III) + H_2O_2 \rightarrow Fe(II) + HO_2^{\bullet} + H^+ \quad (k = 10^{-3} – 10^{-2}\ M^{-1}\ s^{-1}) \quad (2)$$

192 $$Fe(III) + HO_2^{\bullet} \rightarrow Fe(II) + O_2 + H^+ \quad (k = 1 \times 10^4\ M^{-1}\ s^{-1}) \quad (3)$$

In the Fenton and Fenton-like processes, H_2O_2 can assist the Fe(III)/Fe(II) redox cycle, as described in eq 2, while the rate of this reaction is much smaller than that for the formation of $HO^{\bullet}$ via the Haber-Weiss reaction in eq 1. In Fig. 1, the concentration of Fe-Z (109 mg L^{-1}) was smaller than those for the reported systems (500 – 1000 mg L^{-1}) [16-21]. However, when the concentration of Fe-Z was increased to 873 mg L^{-1}, no enhancement in TrBP degradation was detected in the presence of catalyst alone.

To enhance the reduction of Fe(III) to Fe(II) on the surface of the Fe-Z, variety of RAs were tested, as shown in Fig. 1 a – f. All of the RAs enhanced the degradation of TrBP, compared to the case in the presence of the Fe-Z alone (g in Fig. 1). Among these, ASC and NH_2OH (a and f in Fig. 1) were particularly effective RAs in terms of enhancing the degradation of TrBP. Thus, oxidation characteristics of TrBP in the heterogeneous Fenton-like system with the Fe-Z were investigated by focusing on ASC and NH_2OH.

3.3. Optimization of dosages

Figure 2a shows the influence of RA concentration on the percent degradation of TrBP and debromination at pH 3 for a 180 min period. The percent degradation of TrBP and debromination increased with increasing RA concentrations. Although more than 90% of the TrBP and the release of 225 – 270 μM Br^-, corresponding to 2.3 – 2.7 bromine atoms in the degraded TrBP, were observed at concentrations of NH_2OH above 3 mM. However, in the presence of ASC, the maximum percent of TrBP degradation approached, but did not exceed 70%, and the concentration of Br^- reached 120 – 125 μM.

The influence of H_2O_2 concentration on the degradation and debromination of TrBP

were investigated in the presence of 5 mM NH_2OH and 7 mM ASC (Fig. 2b). A 95% degradation of TrBP was achieved at concentrations of H_2O_2 above 2.5 mM, although debromination increased up to 5 mM H_2O_2 and decreased thereafter. Br^- is known to serve as $HO^\bullet$ scavenger ($k < 1\times10^6$ $M^{-1}s^{-1}$) [5]. Thus, the slight decrease in Br^- concentration at concentrations of H_2O_2 above 5 mM may be attributed to the oxidation of Br^-. In the presence of ASC, the percent degradation of TrBP reached a plateau of 60 – 65%, even when a higher concentration of H_2O_2 (100 mM) was used. Based on the experimental data shown in Figs. 2a and b, the following concentrations of RAs and H_2O_2 were determined to be optimal for the degradation of TrBP at 109 mg L^{-1} of Fe-Z: [RA] 5 mM, [H_2O_2] 5 mM for NH_2OH; [RA] 7 mM, [H_2O_2] 20 mM for ASC.

3.4. Influence of Fe-Z concentration on the reaction kinetics

Figure 3 shows the influence of Fe-Z concentration on the kinetics of degradation and debromination of TrBP at pH 3. In the presence of NH_2OH (Fig. 3a and c), the initial rates for degradation and debromination of TrBP increased with an increase in the catalyst concentration, while the initial rates were stagnated above 436 mg L^{-1} of Fe-Z. In the presence of ASC (Fig. 3b and d), the initial rates for degradation and debromination of TrBP also increased with an increase in the catalyst concentration, although the TrBP was not degraded and debrominated completely, even in the higher concentration of the catalyst (827 mg L^{-1}). These results suggest that, in terms of the complete degradation and debromination of TrBP, the addition of ASC is not effective, although NH_2OH is a useful RA. From the experiments of afterword, 436 mg L^{-1} of Fe-Z was selected as the catalyst concentration for the case of NH_2OH to degrade TrBP completely.

241

242 *3.5. Influences of pH on the kinetics of TrBP degradation*

243 Figure 4 shows the influence of kinetics of degradation and debromination by a
244 heterogeneous Fenton-like reaction with the Fe-Z in the presence of NH_2OH (a and c) or
245 ASC (b and d). At pH 3 and 5, TrBP was completely degraded within 60 min and the
246 complete debromination (approximately 300 μM), which corresponds to the release of 3
247 bromine atoms from the degraded TrBP, was observed in the presence of NH_2OH.
248 However, the degradation and debromination of TrBP were retarded at pH 7 (Fig. 4a
249 and c, ▲). In addition, a minor amount of degradation of TrBP and debromination were
250 observed at pH 9 (Fig. 4a and c, ▼). Thus, the effective pH values for debromination
251 and degradation in the presence of NH_2OH were 3 and 5.

252 On the other hand, the pseudo-first-order rate constants for TrBP degradation
253 remained constant in the pH range of 3 – 9 in the presence of ASC (2.0×10^{-2} –
254 2.7×10^{-2} min^{-1}, Fig. 4b and d), while these values were slightly smaller than those at pH
255 3 and 5 in the presence of NH_2OH (6.0×10^{-2} – 6.2×10^{-2} min^{-1}). Although the efficiency
256 of TrBP degradation and debromination were independent of solution pH in the
257 presence of ASC, the percent degradation of TrBP and debromination reached a constant
258 level of 65 – 70% and 100 – 120 μM, respectively. These results indicate that the
259 complete degradation and debromination of TrBP in the presence of added ASC are
260 difficult under any conditions (*i.e.*, concentrations of dosages and pH).

261 The enhanced degradation of TrBP and debromination can be attributed to the
262 reduction of Fe(III) to Fe(II) by RAs on the Fe-Z. NH_2OH is a strong RA, when the
263 solution pH is below its pK_a value (5.94), while the reducing power of NH_2OH is weak
264 above pH 5.94 [28]. Thus, efficient degradation of TrBP and debromination at pH 3 and

5 (Fig. 4a and c) are due to the enhanced reduction of Fe(III) to Fe(II) by NH_2OH. At pH 7 in the presence of NH_2OH, the measured pH in the reaction mixture after a 180 min period was 3.4, while the pH in the reaction mixture at pH 9 decreased to 7.2. Thus, the retardation of TrBP degradation and debromination at pH 7 in the presence of NH_2OH (Fig. 4a and c, ▲) can be attributed to the fact that the reduction of Fe(III) to Fe(II) is initially retarded, and the attack of the generated $HO^{\bullet}$ to TrBP subsequently proceeds when the pH in the reaction mixture decreases. In contrast, ASC can reduce Fe(III) to Fe(II) in a wide pH range [29]. However, the stagnation of TrBP degradation and debromination suggests that the capability for $HO^{\bullet}$ scavenging by ASC is higher than that by NH_2OH.

3.6. Oxidation products and mineralization

The oxidation of bromophenols may produce a variety of brominated quinones and oligomers [32, 40]. Figure 5 shows the GC/MS chromatograms of the extracts from reaction mixtures in the presence of ASC at pH 3, 5, 7 and 9 after a 180-min period. Although no oxidation products were detected at pH 3, the diacetate derivative of 2,6-dibromo-*p*-benzoquinone (2,6DBQ, peak 1) was found as the major byproduct at pH 5, 7 and 9. Based on a standard sample of 2,6DBQ, the percent conversions of the degraded TrBP into 2,6DBQ were estimated to be as follows: pH 5, 20.3%; pH 7, 11.6%; pH 9, 9.0%, decreasing with an increase in pH. Instead of peak 1, peaks 2, 3, 4 and 5 increased at pH 7 and 9. Based on their mass spectra, these peaks were assigned to specific products (Table 2). Although peak 5 was a dimer of TrBP, a more persistent compound, this amount was quite small. In contrast, no peaks corresponding to oxidation products were observed in the presence of NH_2OH at pH 3, 5, 7 and 9 after a

180 min period, suggesting the formation of the degradation of byproducts that are listed in Table 2.

As shown in Fig. 5, only 2,6DBQ was detected as a major intermediate at pH 5. Thus, the kinetic curves of 2,6DBQ formation were compared in the presence of ASC and NH_2OH at pH 5 (Fig. 6). In the presence of NH_2OH, 2,6DBQ formation rapidly increased up to a reaction time of 30 min, decreased thereafter and then disappeared after a 180 min period. In the presence of ASC, the 2,6DBQ concentration increased up to 60 min and then gradually decreased up to 180 min, suggesting that the degradation of 2,6DBQ was incomplete.

It is known that *p*-benzoquinone can be mineralized via oxidative ring-cleavage [26]. Thus, the disappearance of 2,6DBQ may be related to its mineralization. Figure 7a shows the percent mineralization of TrBP and the numbers of bromine atoms released from TrBP during the oxidation reaction at pH 3, 5, 7 and 9 in the presence of NH_2OH after a 180 min period. The percent mineralization decreased with an increase in pH, and no mineralization was observed at pH 9.

For practical use, the degradation in the neutral to weak acid region is preferable. The percents mineralization at pH 5 and 7 were 46% and 23%, respectively, and 0.6 – 0.7% of Fe was eluted from the Fe-Z at pH 5 in the presence of ASC and NH_2OH after a 180 min period. In addition, the catalytic activity for TrBP degradation was maintained after the ten recyclings of Fe-Z, as shown in Supplementary data (Fig. S2). Due to fact the trace amounts of Fe are eluted and the stability of Fe-Z, the sequential addition of NH_2OH and H_2O_2 may be useful method. To achieve the complete mineralization of TrBP, the sequential addition of H_2O_2 and NH_2OH (5 mM) at 180 min intervals was examined (↓ in Fig. 7b). Complete mineralization was achieved after 3 additions of

313 H_2O_2 and NH_2OH.

314

315 *3.7. H_2O_2 consumption*

316 NH_2OH and ASC reduces the Fe(III) on the Fe-Z to produce Fe(II), and H_2O_2 is
317 decomposed by the Fe(II) to produce $HO^\bullet$, as shown in eq 1. However, NH_2OH and
318 ASC can also serve as the $HO^\bullet$ scavengers as follows:

319 $$NH_2OH + HO^\bullet \rightarrow NH_2O^\bullet + H_2O \ (k \leq 5 \times 10^8\ M^{-1}\ s^{-1} \text{ at pH 4 [41]}) \quad (4)$$

320 $$HASC^- + HO^\bullet \rightarrow ASC^{\bullet-} + H_2O \ (k = 1.0 \times 10^{10}\ M^{-1}\ s^{-1}\ [5]) \quad (5)$$

321 In addition, H_2O_2 is regenerated by the disproportionation of $HO^\bullet$ and $HO_2^\bullet$ as follows:

322 $$2HO^\bullet \rightarrow H_2O_2 \ (k = 5.5 \times 10^9\ M^{-1}\ s^{-1}\ [5]) \quad (6)$$

323 $$2HO_2^\bullet \rightarrow H_2O_2 + O_2 \quad (k = 8.5 \times 10^5\ M^{-1}\ s^{-1}\ [36]) \quad (7)$$

324 $$HO_2^\bullet \rightleftharpoons H^+ + O_2^{\bullet-} \quad (pK_a = 4.8\ [36]) \quad (8)$$

325 Although the formation of $HO_2^\bullet$ by the reduction of Fe(III) with H_2O_2 (eq 2) is very
326 slow, the disproportionation of the generated $HO^\bullet$ (eq 6) is fast reaction. Thus, the
327 generated $HO^\bullet$ may be recombined to form H_2O_2, if no scavengers are present. However,
328 H_2O_2 and Fe(II) in the system can serve as $HO^\bullet$ scavengers as follows:

329 $$H_2O_2 + HO^\bullet \rightarrow HO_2^\bullet + H_2O \ (k = 2.7 \times 10^7\ M^{-1}\ s^{-1}\ [5]) \quad (9)$$

330 $$Fe^{2+} + HO^\bullet \rightarrow FeOH^{2+} \quad (k = 4.3 \times 10^8\ M^{-1}\ s^{-1}\ [5]) \quad (10)$$

331 Reactions 1, 2 and 9 are related to the consumption of H_2O_2. Because the concentration
332 of H_2O_2 was much larger than those of Fe(II) and $HO^\bullet$, eq 9 would be dominant
333 reaction for H_2O_2 consumption in the absence of RAs and TrBP. The levels of remained
334 H_2O_2 in the reaction mixture can be determined by the balance between consumption
335 and recombination. The consumption of H_2O_2 may be enhanced in the presence of RAs
336 and TrBP, because $HO^\bullet$ recombination in eq 6 is suppressed. To verify this, the kinetics

of H_2O_2 consumption were examined in the absence and presence of RAs and TrBP.

Figure 8 shows the consumption of H_2O_2 at pH 3 and 9 in the presence of ASC and NH_2OH. Even in the absence of TrBP (▲ and ■), H_2O_2 underwent decomposition at pH 3, compared to that in the presence of Fe-Z alone (Fig. 8a, ×). H_2O_2 was largely consumed at pH 9 in the presence of ASC, while no H_2O_2 decomposition was observed for the case of NH_2OH (Fig. 8b, ▲). At pH 3 in the presence of NH_2OH alone (Fig. 8a, ▲), a slight decomposition of H_2O_2 was observed up to 60 min, while decomposition was enhanced thereafter. The small decrease in H_2O_2 concentration is due to the scavenging of $HO^{\bullet}$ by H_2O_2 and Fe(II), and the increased Fe(II) may mainly serves as a $HO^{\bullet}$ scavenger after 60 min. The fact that no decomposition of H_2O_2 occurred at pH 9 in the presence of NH_2OH alone (Fig. 8b, ▲) can be attributed to the fact that Fe(III) is not reduced to Fe(II) in weakly alkaline pH [28]. The larger decomposition rate of H_2O_2 in the presence of ASC at pH 3 and 9 (Fig. 8, ■) demonstrates the capability of ASC for scavenging $HO^{\bullet}$, which is much larger than that for NH_2OH, consistent with eqs 4 and 5.

When the TrBP was added to the reaction mixture at pH 3 in the presence of NH_2OH, the H_2O_2 rapidly decomposed (Fig. 8a, Δ), compared to the kinetic curve without TrBP (Fig. 8a, ▲). In contrast, the kinetics in the presence of ASC (Fig. 8a, ■ and □) were unchanged, even when TrBP was added. These results indicate that the efficiency of NH_2OH for scavenging $HO^{\bullet}$ is much lower than that of TrBP and the oxidation of TrBP is the dominant reaction in the presence of NH_2OH.

3.8. Analysis of Fe on the Fe-Z by XPS

To elucidate the effect of RAs on the enhancement in Fenton degradation, the states of

361 Fe(III) on the surface of the Fe-Z were compared before and after treating with ASC.
362 The ASC-treated Fe-Z was readily oxidized to Fe(III) under aerobic conditions. Thus,
363 after treating the Fe-Z with the ASC, the sample was immediately transferred to a
364 vacuum desiccator and dried in vacuo. The sample was stored in the desiccators until
365 XPS spectra were obtained. Figure 9 shows the $Fe(2p)_{3/2}$ core-level XPS spectra for
366 Fe-Z before (a) and after treatment with ASC (b). The BEs for Fe(III) and Fe(II) species
367 appear at 710.7 eV and 708.1 eV, respectively, based on those for magnetite (Fe_3O_4),
368 which is a mixture of Fe(III) and Fe(II). The peak components for Fe(III) and Fe(II) in
369 Fe-zeolite are close to one another (711.6 – 712.5 eV for Fe(III) and 709.9 – 710.4 eV
370 for Fe(II)) [42]. Thus, waveform analyses were carried out for the $Fe(2P)_{3/2}$ peaks. The
371 rates of Fe(III) and Fe(II) components before and after treatment with ASC were
372 estimated as follows: before the reaction, 100% Fe(III), 0% Fe(II); after ASC treatment,
373 82% Fe(III), 18% Fe(II). These values confirm that RAs such as ASC can assist the
374 Fe(III)/Fe(II) redox cycle to enhance the generation of $HO^{\bullet}$.
375
376 *3.9. Significance in application*
377 Adding NH_2OH to a heterogeneous Fenton-like system with the Fe-Z was more
378 advantageous than the addition of ASC, in terms of the complete mineralization of TrBP.
379 For the case of NH_2OH, the end products of the reduction of Fe(III) are N_2, N_2O, NO_3^-
380 and NO_2^- [28]. At pH 3 and 5, approximately 30% of the NH_2OH was converted into
381 NO_3^- and NO_2^- after a 180 min reaction period, as shown in Supplementary data (Fig.
382 S3). However, the formation of NO_3^- and NO_2^- is not desirable, and they should be
383 removed before being sent to an aquatic environment by combining this process with an
384 additional treatment technique (e.g., microbial treatment [42]). NH_2OH is commercially

385 available as a 50% (*ca*. 15 M) aqueous solution (CAS No. 7803-49-8). As shown in Fig.
386 6b, three additions of 5 mM NH_2OH is required to completely mineralize TrBP.
387 Approximately 1 L of a 50% aqueous NH_2OH is required for the treatment of 1 m^3 of
388 wastewater. This may be a reasonable amount and suggests that such a system might be
389 applicable for the treatment of wastewater.
390
391 **4. Conclusions**
392 Fe(II) was loaded onto the cation-exchange sites in a natural zeolite, and was strongly
393 bound as the Fe(III) ionic form after calcination at 773 K. Although the prepared Fe-Z
394 was not effective for the oxidation of TrBP via a Fenton-like process, the addition of
395 ASC or NH_2OH resulted in a significant enhancement in the degradation and
396 debromination of TrBP. The kinetics of TrBP degradation and H_2O_2 consumption
397 indicate that ASC serves as a strong $HO^{\bullet}$ scavenger at any pH and leads to the
398 incomplete degradation of TrBP. Thus, ASC was not an effective RA for the enhanced
399 degradation and debromination of TrBP. In contrast, the complete degradation and
400 debromination of TrBP could be achieved at pH 3 and 5 in the presence of NH_2OH,
401 indicating that this RA is a suitable additive for enhancing heterogeneous Fenton-like
402 oxidation reactions using Fe-Z. In addition, TrBP was completely mineralized at pH 5
403 after the sequential addition of H_2O_2 and NH_2OH. The role of RAs are to enhance the
404 reduction of Fe(III) on the Fe-Z to Fe(II), which permits the generation of $HO^{\bullet}$ to be
405 accelerated via the Haber Weiss reaction.
406
407 **Acknowledgment**
408 This work was supported by Grants-in-Aid for Scientific Research from Japan Society

for Promotion of Science (25241017).

References

[1] W.-J. Sim, S.-H. Lee, I.-S. Lee, S.-D. Choi, J.-E. Oh, Chemosphere 77 (2009) 552-558.

[2] I.A.T.M. Meerts, J.J. Zanden, E.A.C. Luijuks, I. van Leeuwen-Bol, G. Marsh, E. Jakobsson, A. Bergman, A. Brouwer, Toxicol. Sci. 56 (2000) 95-104.

[3] M. Fukushima, Y. Mizutani, S. Maeno, Q. Zhu, H. Kuramitz, S. Nagao, Molecules 17 (2012) 48-60.

[4] F. Haber, J. Weiss, Naturwissenschaften 20 (1932) 948-950.

[5] G.V. Buxton, C.L. Greenstock, W.P. Helman, A.B. Ross, J. Phys. Chem. Ref. Data 17 (1988) 513-886.

[6] M. Pera-Titus, V. García-Molina, M.A. Baños, J. Giménez, S. Esplugas, Appl. Catal. B-Environ. 47 (2004) 219-256.

[7] M. Fukushima, K. Tatsumi, Environ. Sci. Technol. 35 (2001) 1771-1778.

[8] M. Fukushima, K. Tatsumi, K. Morimoto, Environ. Toxicol. Chem. 19 (2000) 1711-1716.

[9] M.A. Tarr, in: Tarr, M.A. (Ed.), Chemical Degradation Methods for Wastes and Pollutants – Environmental and Industrial Applications. Dekker, New York, 2003, pp. 165-200.

[10] L. Xu, J. Wang, Appl. Catal. B-Environ. 123-124 (2012) 117-126.

[11] J.H. Ramirez, C.A. Costa, L.M. Madeira, G. Mata, M.A. Vicente, M.L. Rojas-Cervantes, A.J. López- Peinado, R.M. Martín-Aranda, Appl. Catal. B-Environ. 71 (2007) 44–56.

433 [12] M.N. Timofeeva, S.T. Khankhasaeva, Y.A. Chesalov, S.V. Panchenko, V.N.
434 Tsybulya, E.T. Panchenko, Dashinamzhilova, Appl. Catal. B-Environ. 88 (2009)
435 127–134.
436 [13] J. Herney-Ramirez, M.A. Vicente, L.M. Madeira, Appl. Catal. B-Environ. 98
437 (2010) 10-26.
438 [14] R.-M. Liou, S.-H. Chen, M.-Y. Hung, C.S. Hsu, Chemosphere 55 (2004)
439 1271-1280.
440 [15] R.- M. Liou, S.-H. Chen, M.-Y. Hung, C.S. Hsu, J.-Y. Lai, Chemosphere 59 (2005)
441 117-125.
442 [16] S. Navalon, M. Alvaro, H. Garcia, Appl. Catal. B-Environ. 99 (2010) 1-26.
443 [17] M. Neamțu, C. Zaharia, C. Catrinescu, A. Yediler, M. Macoveanu, A. Kettrup, Appl.
444 Catal. B-Environ. 48 (2004) 287-294.
445 [18] M. Neamțu, C. Catrinescu, A. Kettrup, Appl. Catal. B-Environ. 51 (2004) 149-157.
446 [19] W. Najjar, S. Azabou, S. Sayadi, A. Ghorbed, Appl. Catal. B-Environ. 88 (2009)
447 299-304.
448 [20] R. Gonzalez-Olmos, M. Martin, A. Georgi, F.-D. Kopinke, I. Oller, Appl. Catal.
449 B-Environ. 125 (2012) 51-58.
450 [21] R. Gonzalez-Olmos, F. Holzer, F.-D. Kopinke, A. Georgi, Appl. Catal. A-Gen. 398
451 (2011) 44-53.
452 [22] S. Wang, Z.H. Zhu, J. Hazard. Mater. B318 (2006) 946-952.
453 [23] A. Miura, R. Okabe, K. Izumo, M. Fukushima, Appl. Clay Sci. 46 (2009) 277-282.
454 [24] S. Fukuchi, A. Miura, R. Okabe, M. Fukushima, M. Sasaki, T. Sato, J. Mol. Struct.
455 982 (2010) 181-186.
456 [25] S. Fukuchi, M. Fukushima, R. Nishimoto, G. Qi, T. Sato, Clay Miner. 47 (2012)

457 355-364.
458 [26] M. Fukushima, K. Tatsumi, K. Morimoto, Environ. Sci. Technol. 34 (2000)
459 2006-2013.
460 [27] C.A. Martínez-huitle, E. Brillas, Appl. Catal. B-Environ. 87 (2009) 105-145.
461 [28] L. Chen, J. Ma, X. Li, J. Zhang, J. Fang, Y. Guan, P. Xie, Environ. Sci. Technol. 45
462 (2011) 3925-3930.
463 [29] Y. Li, T. Zhu, J. Zhao, B. Xu, Environ. Sci. Technol. 46 (2012) 10304-10309.
464 [30] M. Fukushima, M. Kawasaki, A. Sawada, H. Ichikawa, K. Morimoto, K. Tatsumi,
465 S. Tanaka, J. Mol. Catal. A-Chem. 187 (2002) 201-213.
466 [31] M. Fukushima, S. Tanaka, K. Nakayasu, K. Sasaki, K. Tatsumi, Anal. Sci. 15
467 (1999) 185-188.
468 [32] S. Shigetatsu, M. Fukushima, S. Nagao, J. Environ. Sci. Heal. A 45 (2010)
469 1536-1542.
470 [33] M. Fukushima, K. Tatsumi, Talanta 47 (1998) 899-905.
471 [34] K. Elaiopoulos, Th. Perraki, E. Grigoropoulou, Micropor. Mesopor. Mat. 112
472 (2008) 441-449.
473 [34] R.J. Reiter, D.-x. Tan, L.C. Manchester, W. Qi, Cell Biochem. Biophys. 34 (2001)
474 237-256.
475 [35] R. Chen, J.J. Pignatello, Environ. Sci. Technol. 31 (1997) 2399-2406.
476 [36] M. Fukushima, K. Tatsumi, Colloid Surf. A-Physicochem. Eng. Asp. 155 (1999)
477 249-258.
478 [37] Y. Zuo, J. Hoigné, Environ. Sci. Technol. 26 (1992) 1014-1022.
479 [38] H. Iwai, M. Fukushima, M. Yamamoto, Anal. Sci. 29 (2013) 723-728.
480 [39] M. Fukushima, Y. Ishida, S. Shigematsu, H. Kuramitz, S. Nagao, Chemosphere 80

(2010) 860-865.

[40] M. Simic, E. Hayon, J. Am. Chem. Soc. 93 (1971) 5982-5986.

[41] J. Duxiao, H. Nongyue, Z. Yuanying, X. Chunxiang, Y. Chunwei, L. Zuhong, Mater. Chem. Phys. 69 (2001) 246-251.

[42] Z. Shen, Y. Zhou, J. Wang, Bioresource Technol. 131 (2013) 33-39.

Figure captions

Fig. 1. Effects of reducing agents on the kinetics of TrBP degradation. (a) ASC, (b) oxalic acid, (c) *p*-hydroquinone, (d) humic acid, (e) gallic acid, (f) NH_2OH, (g) without RAs, concentrations 50 mg L^{-1} for humic acid and 10 mM for other reducing agents. $[TrBP]_0$ 100 μM, $[H_2O_2]$ 20 mM, Fe-Z 109 mg L^{-1} (30 μM), pH 3.

Fig. 2. Influence of the concentration of RAs (a) and H_2O_2 (b) on TrBP degradation (▲ and ■) and debromination (Δ and □). ▲ and Δ: NH_2OH, ■ and □: ASC. (a) $[TrBP]_0$ 100μM, $[H_2O_2]$ 20 mM, Fe-Z 109 mg L^{-1} (30 μM), 180 min, pH 3; (b) $[TrBP]_0$ 100μM, [RAs] 5 mM for NH_2OH and 7 mM for ASC, Fe-Z 109 mg L^{-1} (30 μM), 180 min, pH 3.

Fig. 3. Influence of the concentration of Fe-Z on the degradation and debromination of TrBP in the presence of NH_2OH (a and c) and ASC (b and d). (a) and (b): Kinetics for TrBP degradation. (c) and (d): Kinetics for debromination. (a) and (c): $[H_2O_2]$ 5 mM, $[NH_2OH]$ 5 mM, pH 3. (b) and (d): $[H_2O_2]$ 20 mM, [ASC] 7 mM, pH 3.

Fig. 4. Kinetic curves for the degradation and debromination of TrBP at pH 3, 5, 7 and 9. Degradation of TrBP in the presence of NH_2OH (a) and ASC (b). Debromination in the presence of NH_2OH (c) and ASC (d). $[TrBP]_0$ 100μM, $[H_2O_2]$ 5 mM for NH_2OH and 20 mM for ASC, [RAs] 5 mM for NH_2OH and 7 mM for ASC, [Fe-Z] 436 mg L^{-1} (240 μM) for NH_2OH and 109 mg L^{-1} (60 μM) for ASC.

510 **Fig. 5.** The GC/MS chromatograms of a hexane extract of the reaction mixture at pH 3,
511 5, 7 and 9 in the presence of ASC. $[TrBP]_0$ 100 μM, $[H_2O_2]$ 20 mM, [ASC] 7 mM, Fe-Z
512 109 mg L^{-1} (30 μM), reaction time 180 min.
513
514 **Fig. 6.** Kinetics of TrBP degradation and 2,6DBQ formation at pH 5 in the presence of
515 NH_2OH (▲ and Δ) or ASC (■ and □). $[TrBP]_0$ 100μM, $[H_2O_2]$ 5 mM for NH_2OH and
516 20 mM for ASC, [RAs] 5 mM for NH_2OH and 7 mM for ASC, [Fe-Z] 436 mg L^{-1} (240
517 μM) for NH_2OH and 109 mg L^{-1} (60 μM) for ASC.
518
519 **Fig. 7.** Influence of pH on the percent mineralization and numbers of bromine atoms
520 released from TrBP after a 180 min period (a), and the variations in the percent
521 mineralization at pH 5 by the sequential addition of H_2O_2 and NH_2OH for every 180
522 min (b). $[TrBP]_0$ 100 μM, $[H_2O_2]$ 5 mM, $[NH_2OH]$ 5 mM, [Fe-Z] 436 mg L^{-1} (240 μM).
523
524 **Fig. 8.** Kinetics of H_2O_2 decomposition at pH 3 (a) and 9 (b). Without RAs (×), NH_2OH
525 alone (▲), ASC alone (■), NH_2OH + TrBP (Δ) and ASC + TrBP (□). $[TrBP]_0$ 100μM,
526 $[H_2O_2]$ 5 mM for NH_2OH and 20 mM for ASC, [RAs] 5 mM for NH_2OH and 7 mM for
527 ASC, [Fe-Z] 436 mg L^{-1} (240 μM) for NH_2OH and 109 mg L^{-1} (60 μM) for ASC.
528
529 **Fig. 9.** $Fe(2p)_{3/2}$ core-level XPS spectrum of the Fe-Z before (a) and after treatment with
530 ASC (b). Conditions for the treatment: pH 9; ASC 10 mM; Fe-Z 200 mg L^{-1}; reaction
531 time, 180 min.

Table 1. Inorganic element content, cation exchange capacity (CEC), specific surface area (SSA), total pore volume and average pore diameter for original zeolite and Fe-Z.

Sample	Inorganic elements (%)				CEC ($cmol\ kg^{-1}$)	SSA ($m^2\ g^{-1}$)	Total pore volume ($cm^3\ g^{-1}$)	Average pore diameter (nm)
	Al	Si	Ca	Fe				
Original zeolite	2.5±0.46	40.8±5.7	21.4±1.4	0.49±0.05	150±22	33.3	0.108	13
Fe-Z	2.38±0.22	38.9±0.02	14.9±0.2	1.54±0.06	71.7±6.1	26.2	0.131	20

Table 2. Mass spectral assignments for oxidation products corresponding to peaks 1 - 5 in Fig. 4.

Peak No.	m/z [rel. int., fragment identity]	Assigned structures
1	325 [1.02, M^+], 310 [7.75, $(M - CH_2CO)^+$], 268 [34.15, $(M - 2CH_2CO)^+$]	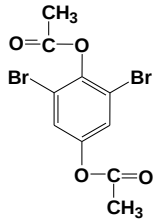
2	430 [1.24, M^+], 388 [4.46, $(M - CH_2CO)^+$], 346 [30.47, $(M - 2CH_2CO)^+$]	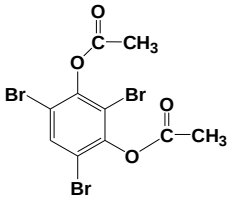
3	410 [1.44, M^+], 368 [3.57, $(M - CH_2CO)^+$], 326 [12.67, $(M - 2CH_2CO)^+$], 284 [17.29, $(M - 3CH_2CO)^+$]	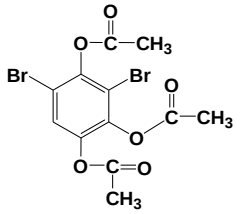
4	450 [1.52, M^+], 408 [9.22, $(M - CH_2CO)^+$], 366 [33.52, $(M - 2CH_2CO)^+$], 349 [30.32, $(M - (CH_2CO)_2OH)^+$]	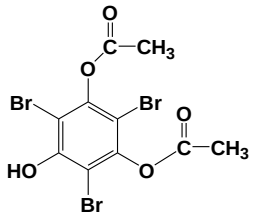
5	586 [8.18, M^+], 544 [29.53, $(M - CH_2CO)^+$], 527 [16.36, $(M - OCOCH_3)^+$], 505 [2.06, M - HBr], 293 [2.07, $C_6H_2OBr_2CH_2CO)^+$]	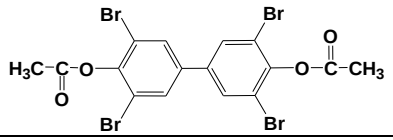

Figure(s)

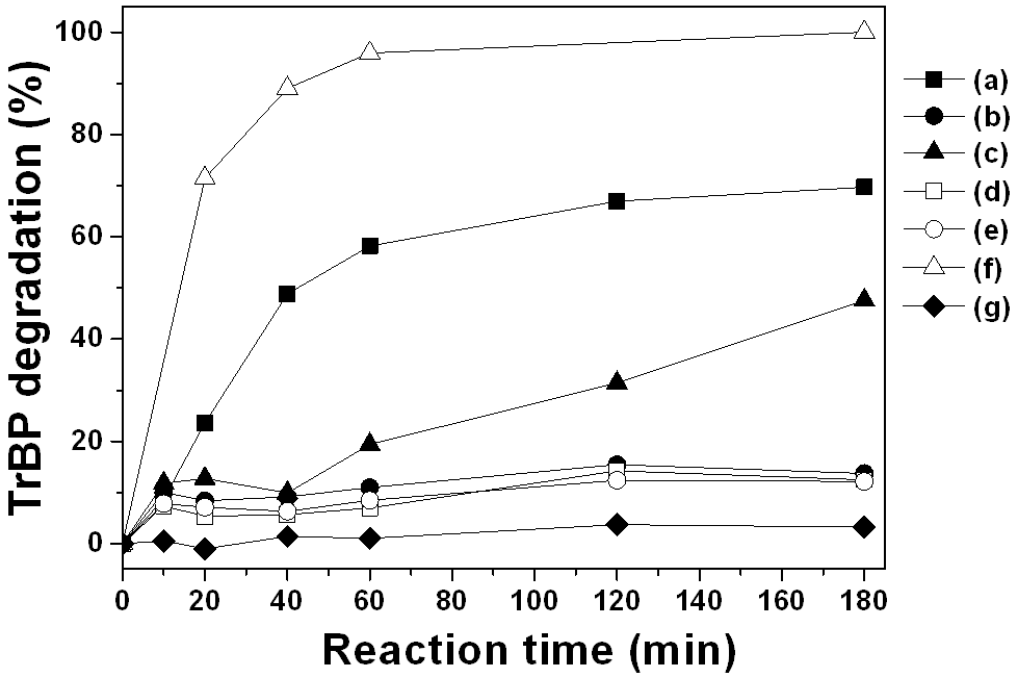

Fig. 1 (APCATB-D-13-00189R2)

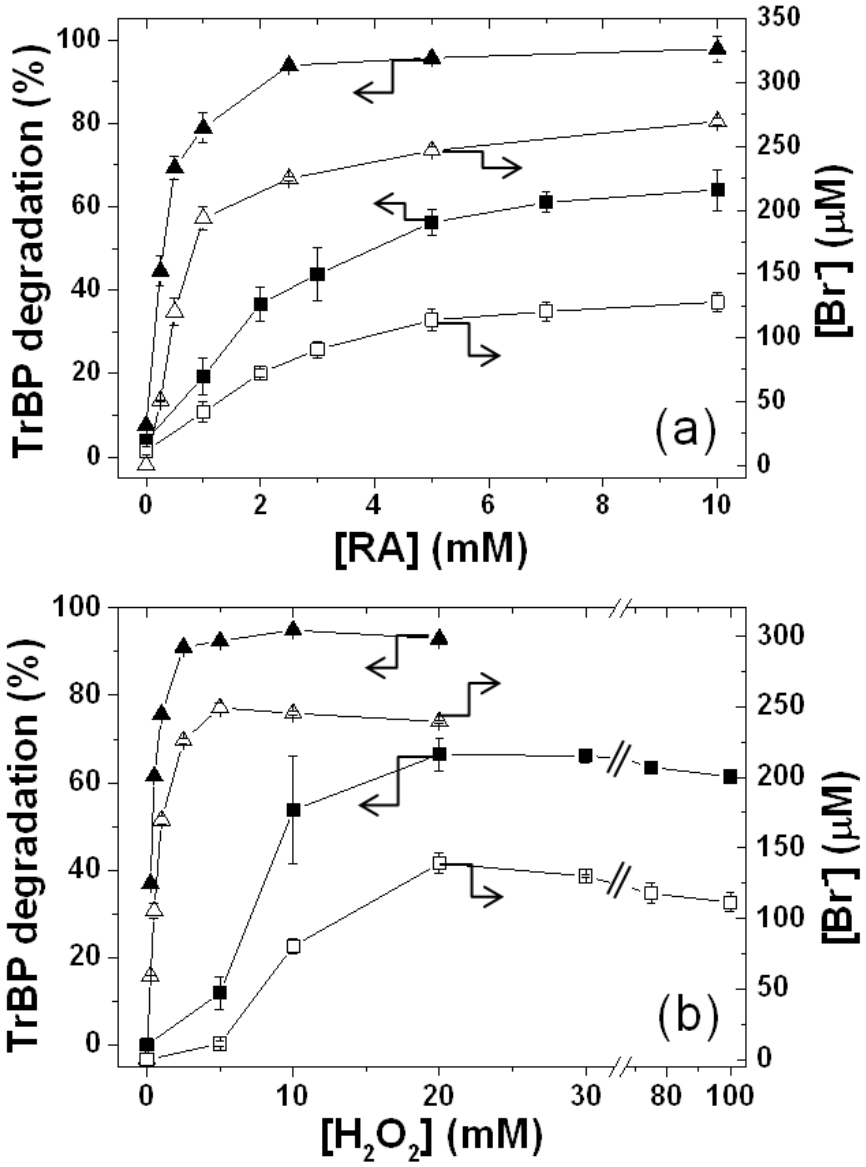

Fig. 2 (APCATB-D-13-00189R2)

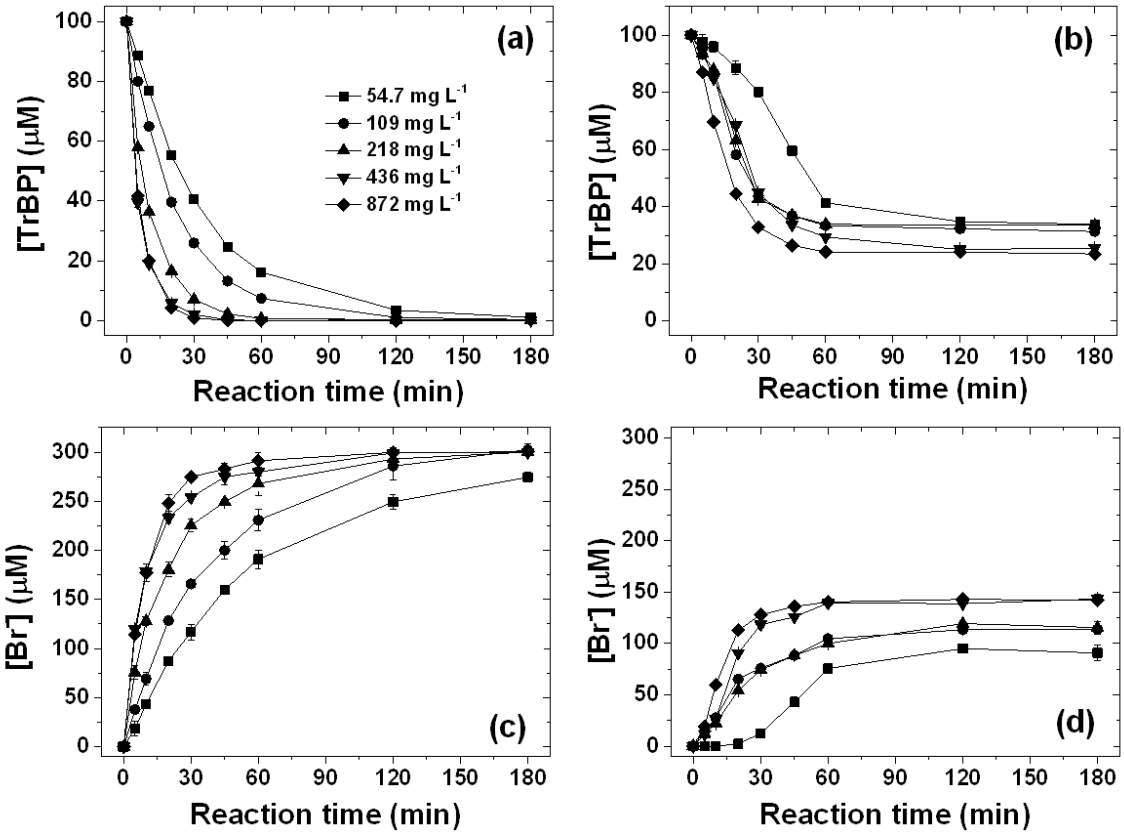

Fig. 3 (APCATB-D-13-00189R2)

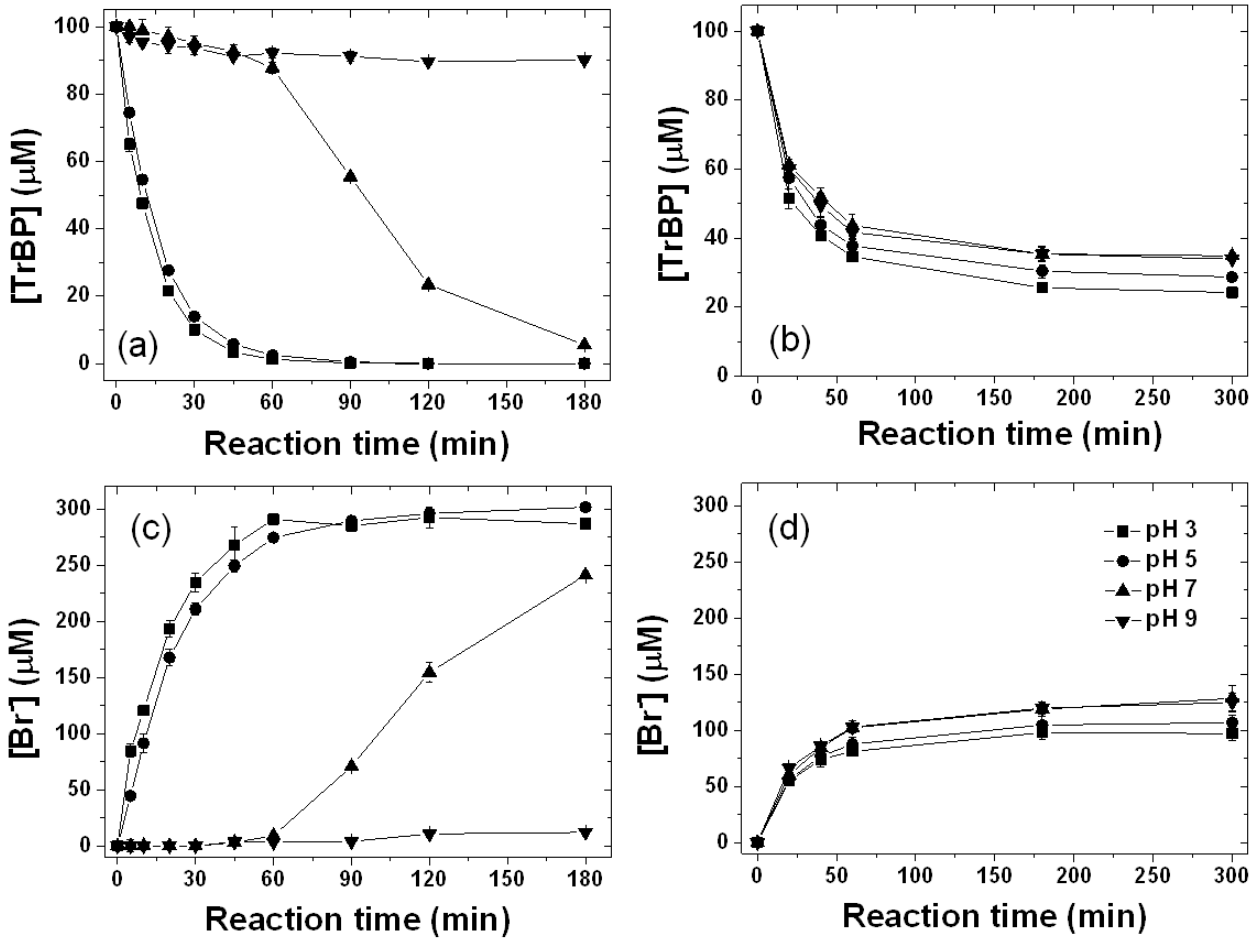

Fig. 4 (APCATB-D-13-00189R2)

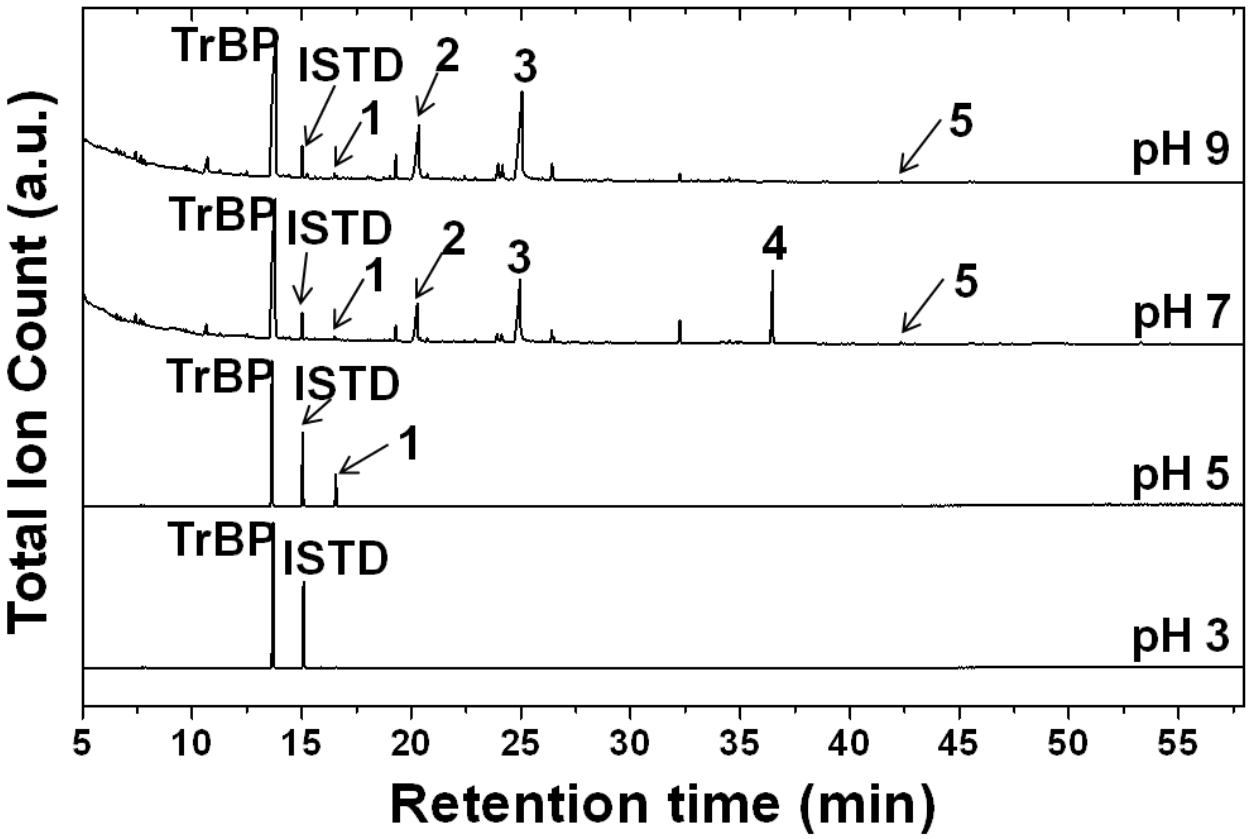

Fig. 5 (APCATB-D-13-00189R2)

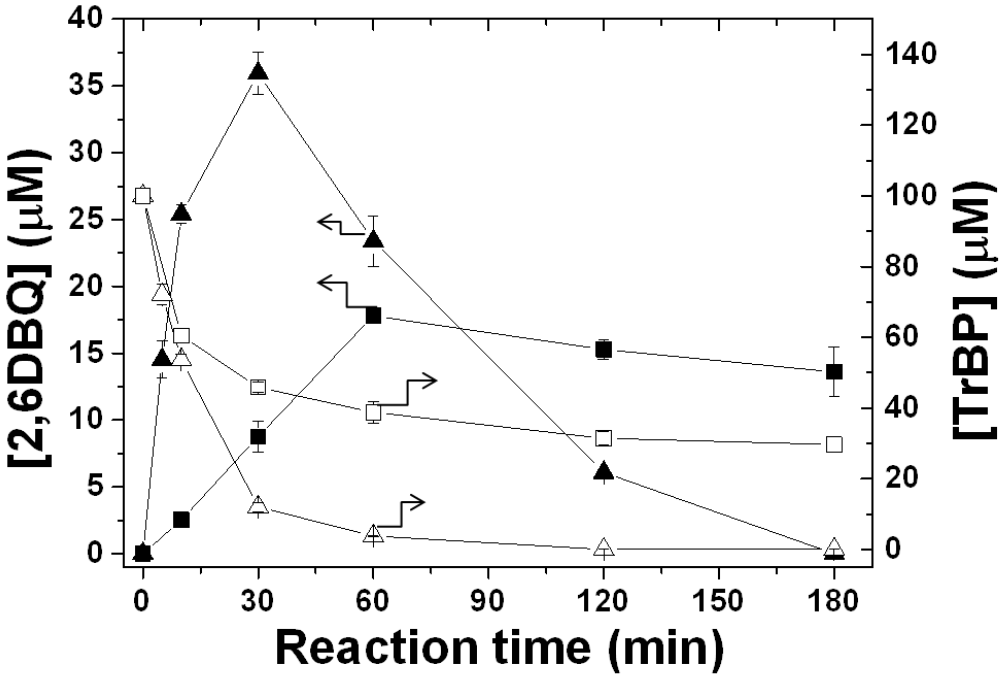

Fig. 6 (APCATB-D-13-00189R2)

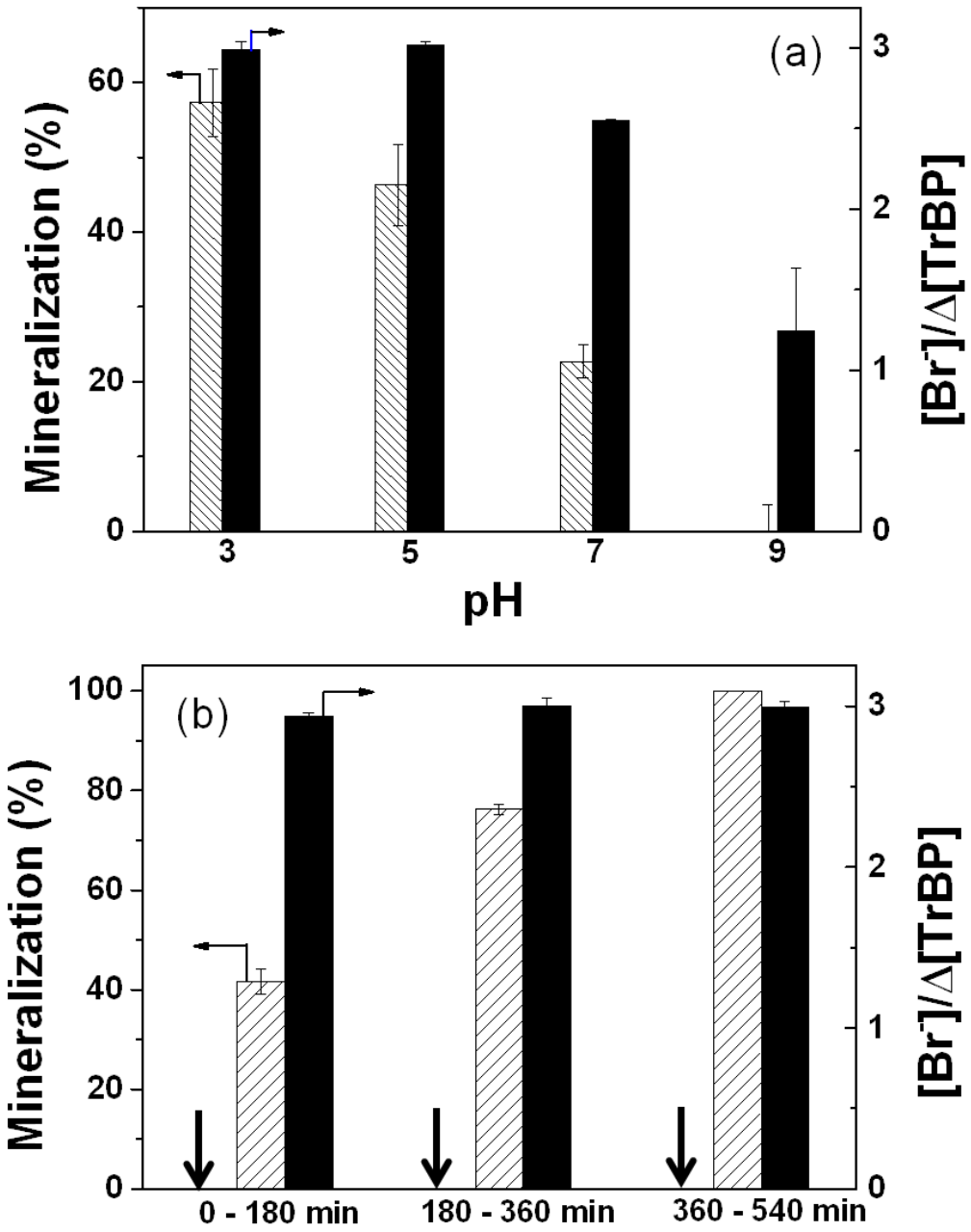

Fig. 7 (APCATB-D-13-00189R2)

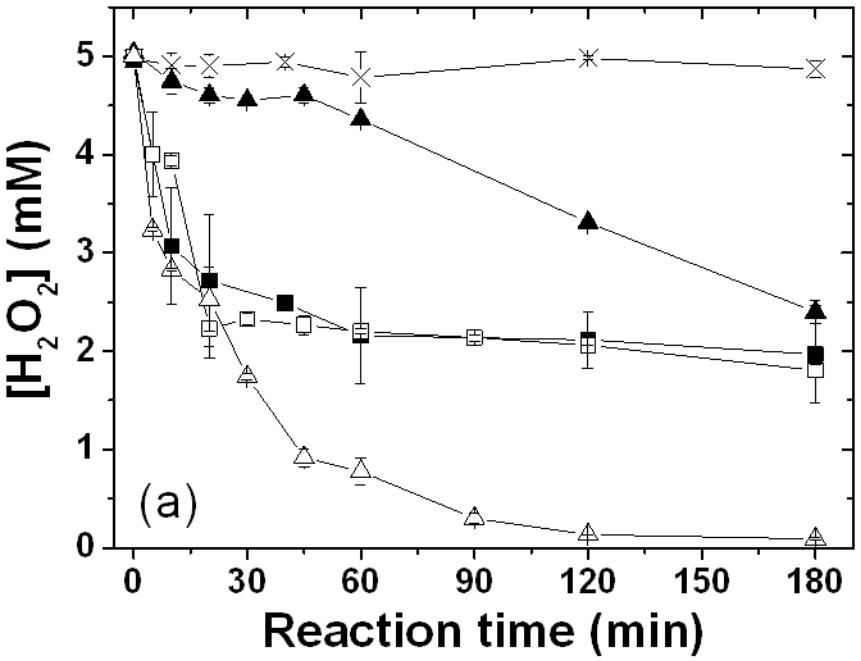

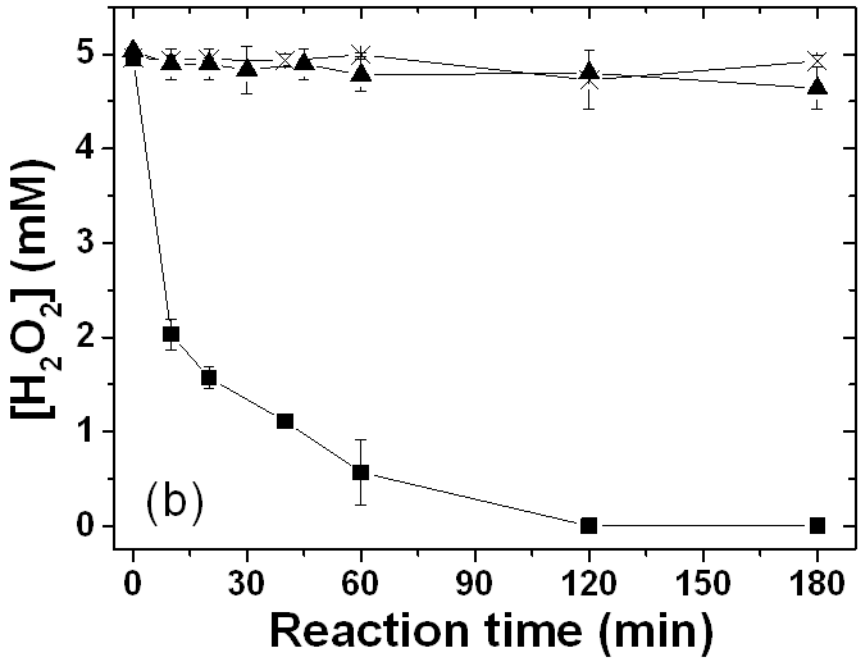

Fig. 8 (APCATB-D-13-00189R2)

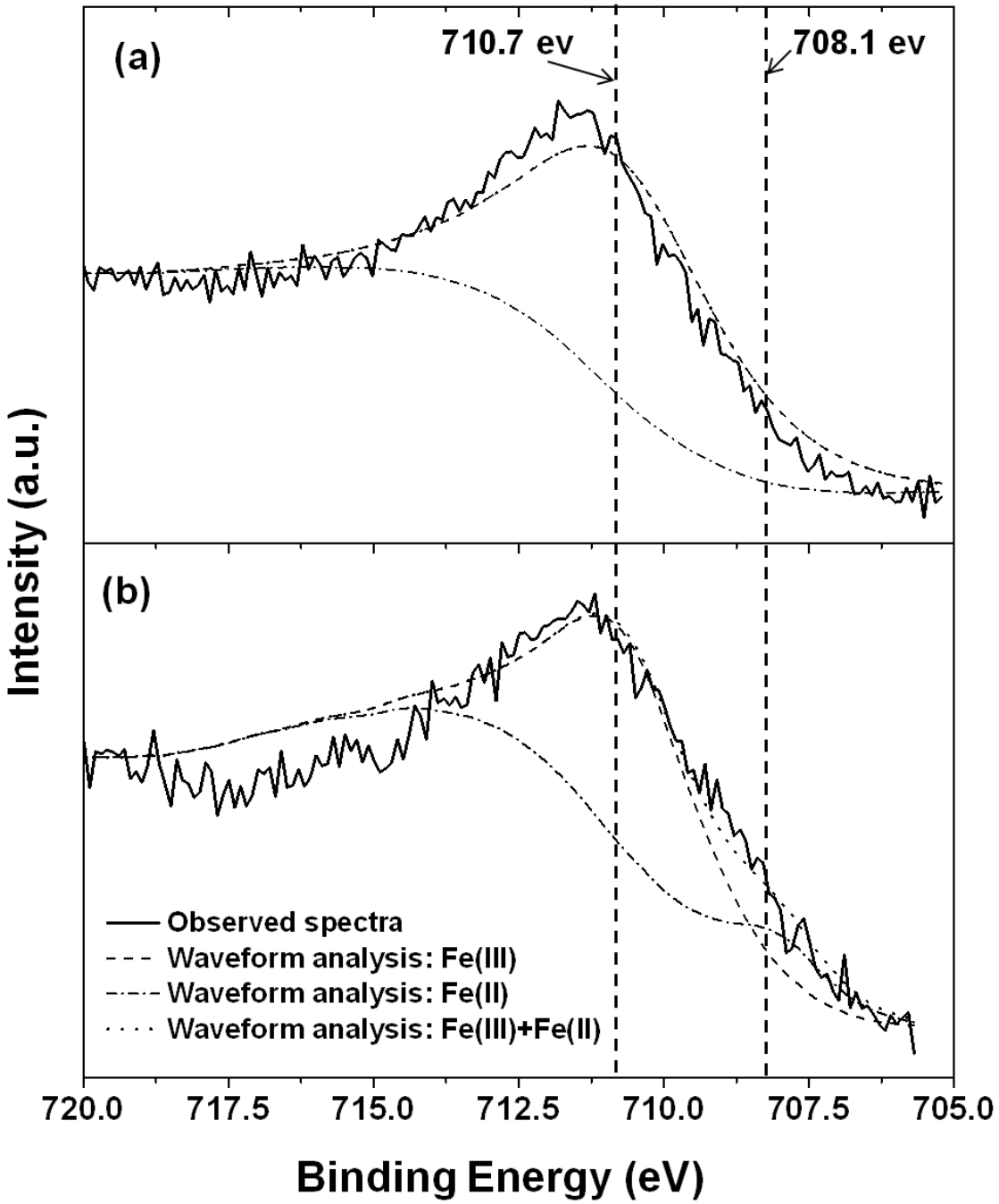

Fig. 9 (APCATB-D-13-00189R2)

Graphical Abstract

Effects of reducing agents on the degradation of 2,4,6-tribromophenol in a heterogeneous Fenton-like system with an iron-loaded natural zeolite

Shigeki Fukuchi, Ryo Nishimoto, Masami Fukushima and Qianqian Zhu

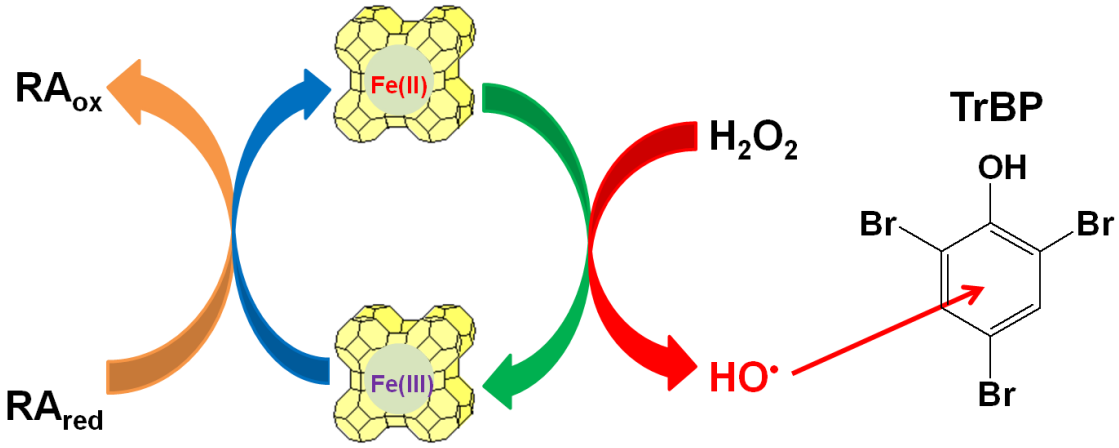

Highlights

Effects of reducing agents on the degradation of 2,4,6-tribromophenol in a heterogeneous Fenton-like system with an iron-loaded natural zeolite

Shigeki Fukuchi, Ryo Nishimoto, Masami Fukushima and Qianqian Zhu

< An Fe-loaded natural zeolite was applied to oxidize TrBP via a Fenton-like process. <

Catalytic activity of the prepared catalyst was not so high for TrBP degradation. <

Addition of NH_2OH resulted in the complete degradation of TrBP at pH 3 and 5. <

Sequential addition of the dosages led to complete mineralization of TrBP at pH 5. <